

Sensitization of titanium dioxide and strontium titanate electrodes by ruthenium(II) tris(2,2'-bipyridine-4,4'-dicarboxylic acid) and zinc tetrakis(4-carboxyphenyl)porphyrin: an evaluation of sensitization efficiency for component photoelectrodes in a multipanel device

Reza Dabestani, Allen J. Bard, Alan Campion, Marye Anne Fox, Thomas E. Mallouk, Stephen E. Webber, and J. M. White

J. Phys. Chem., **1988**, 92 (7), 1872-1878 • DOI: 10.1021/j100318a035

Downloaded from <http://pubs.acs.org> on February 2, 2009

More About This Article

The permalink <http://dx.doi.org/10.1021/j100318a035> provides access to:

- Links to articles and content related to this article
- Copyright permission to reproduce figures and/or text from this article

Sensitization of Titanium Dioxide and Strontium Titanate Electrodes by Ruthenium(II) Tris(2,2'-bipyridine-4,4'-dicarboxylic acid) and Zinc Tetrakis(4-carboxyphenyl)porphyrin: An Evaluation of Sensitization Efficiency for Component Photoelectrodes in a Multipanel Device

Reza Dabestani, Allen J. Bard, Alan Campion, Marye Anne Fox,* Thomas E. Mallouk, Stephen E. Webber, and J. M. White

Department of Chemistry, University of Texas, Austin, Texas 78712 (Received: December 1, 1986; In Final Form: October 6, 1987)

The utility of polycrystalline anatase TiO_2 and SrTiO_3 semiconductor electrodes sensitized by ruthenium(II) tris(2,2'-bipyridine-4,4'-dicarboxylic acid) (**1**) and by zinc tetrakis(4-carboxyphenyl)porphyrin (**2**) as component photoelectrodes in a multipanel array has been evaluated. The efficiency for photocurrent generation of a single sensitized electrode is decreased as the sensitizer loading on the surface is increased beyond monolayer coverage. Power curves for both sensitizers were obtained in aqueous solutions of potassium iodide, hydroquinone, hydroquinonesulfonate (potassium salt), durohydroquinone, and potassium ferrocyanide as electron donors. From stability and efficiency considerations, hydroquinone is the most appropriate electron donor among this group. The maximum quantum efficiency attained on the metal oxide coated electrodes described herein for monochromatic excitation of **1** was 41% on TiO_2 (surface coverage 3.0×10^{-10} mol/cm²) and 57% on SrTiO_3 (surface coverage 5.9×10^{-11} mol/cm²). With **2** at 420 nm a maximum quantum efficiency on TiO_2 was 9.5% (surface coverage 1.7×10^{-10} mol/cm²) and on SrTiO_3 was 27% (surface coverage 5.0×10^{-12} mol/cm²). Better efficiencies were observed with adsorbed than with chemically bonded **1**. The quantitative reproducibility of the observed photocurrents was a sensitive function of the preparation and porosity of the metal oxide surface. Porous TiO_2 gave better photoresponse than photodoped SrTiO_3 as a photosensitized electrode. Despite these relatively high quantum efficiencies, the steady-state photocurrents produced on these sensitized electrodes were too low for practical operation in a multipanel device.

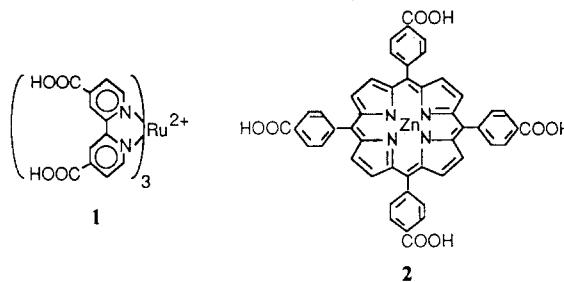
Introduction

We have recently described a multipanel photoelectrochemical device capable of unassisted water splitting.¹ The practical utility of a device constructed with TiO_2/Pt photoelectrodes for solar energy conversion is limited, however, by TiO_2 's lack of absorption of visible wavelengths. This problem could be solved if an efficient sensitizer responsive to incident visible light could be identified.

Spectral sensitization of wide-band-gap semiconductors has been the subject of intensive investigation in recent years.² Chromophores such as xanthene dyes,³ ruthenium complexes,⁴ and

metalloporphyrins⁵ have been reported to sensitize metal oxides, initiating water cleavage. A recent report by Graetzel et al.⁶ was particularly encouraging, with a 44% incident photon-to-current efficiency for charge injection to TiO_2 from adsorbed, excited ruthenium(II) tris(2,2'-bipyridine-4,4'-dicarboxylic acid) reported.

We report here quantum efficiencies for sensitization of TiO_2 and SrTiO_3 by ruthenium(II) tris(2,2'-bipyridine-4,4'-dicarboxylic acid) (**1**) and zinc tetrakis(4-carboxyphenyl)porphyrin (**2**), the



(1) (a) Smotkin, E.; Bard, A. J.; Campion, A.; Fox, M. A.; Mallouk, T.; Webber, S. E.; White, J. M. *J. Phys. Chem.* **1986**, *90*, 4604. (b) Smotkin, E.; Cervera-March, S.; Bard, A. J.; Capion, A.; Fox, M. A.; Mallouk, T.; Webber, S. E.; White, J. M. *Ibid.* **1987**, *91*, 6.

(2) (a) Gerischer, H.; Michel-Beyerle, M. E.; Rebentrost, F.; Tributsch, H. *Electrochim. Acta* **1968**, *13*, 1509. (b) Tributsch, H. *Ber. Bunsen.-Ges. Phys. Chem.* **1969**, *73*, 582. (c) Nemba, S.; Hishiki, Y. *J. Phys. Chem.* **1965**, *69*, 724. (d) Gerischer, H. In *Physical Chemistry: An Advanced Treatise*; Academic: New York, 1970; Vol. IX A. (e) Tributsch, H.; Calvin, M. *Photochem. Photobiol.* **1971**, *14*, 95. (f) Memming, R. *Ibid.* **1972**, *16*, 325. (g) Memming, R.; Tributsch, H. *J. Phys. Chem.* **1971**, *75*, 565. (h) Fujishima, A.; Watanabe, T.; Tatsuki, O.; Honda, K. *Chem. Lett.* **1975**, *13*. (i) Gerischer, H. *Photochem. Photobiol.* **1975**, *16*, 243. (j) Matsumura, M.; Nomura, Y.; Tsubomura, H. *Bull. Chem. Soc. Jpn.* **1976**, *49*, 1409. (k) Clark, W. D. K.; Sutin, N. *J. Am. Chem. Soc.* **1977**, *99*, 4676. (l) Hamnett, A.; Dare-Edwards, M. P.; Wright, R. D.; Seddon, K. R.; Goodenough, J. B. *J. Phys. Chem.* **1979**, *82*, 3280. (m) Memming, R. *Surf. Sci.* **1980**, *101*, 551. (n) Turasaki, T.; Sawada, T.; Kamada, H.; Fujishima, A.; Honda, K. *J. Phys. Chem.* **1979**, *83*, 2142. (o) Krishnan, M.; Zhang, X.; Bard, A. J. *J. Am. Chem. Soc.* **1984**, *106*, 7371, and references cited therein. (p) Chang, B. T.; Campet, G.; Claverie, J.; Hangenmuller, P. *Bull. Chem. Soc. Jpn.* **1984**, *57*, 2574. (q) Wrighton, M. S.; Ellis, A. B.; Wolczanski, P. T.; Morse, D. L.; Abrahamson, H. B.; Ginley, D. S. *J. Am. Chem. Soc.* **1976**, *98*, 2774. (r) Odekerk, B.; Blakemore, J. S. *J. Electrochem. Soc.* **1983**, *130*, 321.

(3) (a) Kalyanasundaram, K.; Dung, D. *J. Phys. Chem.* **1980**, *84*, 2551. (b) Chang, M. S.; Bolton, J. R. *Photochem. Photobiol.* **1981**, *34*, 537. (c) Misawa, H. H.; Sakuragi, Y.; Usui; Tokumaru, K. *Chem. Lett.* **1983**, 1021. (d) Hashimoto, K.; Kawai, T.; Sakata, T. *Ibid.* **1983**, 709. (e) Mau, A. W.; Johansen, O.; Sasse, W. H. F. *Photochem. Photobiol.* **1985**, *41*, 503. (f) Shimidzu, T.; Iyodo, T.; Koide, Y. *J. Am. Chem. Soc.* **1985**, *107*, 35. (g) Sonntag, L. P.; Spittler, M. T. *J. Phys. Chem.* **1985**, *89*, 1453.

(4) (a) Fujihira, M.; Oshih, N.; Osa, T. *Nature (London)* **1977**, *268*, 226. (b) Spittler, M. T.; Calvin, M. *J. Chem. Phys.* **1977**, *66*, 4294. (c) Andersson, S.; Constable, E. C.; Dare-Edwards, M. P.; Goodenough, J. B.; Hamnett, A.; Seddon, K. R.; Wright, R. D. *Nature (London)* **1979**, *280*, 571. (d) Fan, F. R.; Bard, A. J. *J. Am. Chem. Soc.* **1979**, *101*, 6139. (e) Dare-Edwards, M. P.; Goodenough, J. B.; Hamnett, A.; Seddon, K. R.; Wright, R. D. *Faraday Discuss. Chem. Soc.* **1980**, No. 70, 285. (f) Giraudeau, A.; Fan, F. R.; Bard, A. J. *J. Am. Chem. Soc.* **1980**, *102*, 5137. (g) Hishimoto, K.; Kawai, T.; Sakata, T. *Nouv. J. Chim.* **1983**, *7*, 249. (h) Matsumura, M.; Mitsuda, K.; Yoshizaura, N.; Tsubomura, H. *Bull. Chem. Soc. Jpn.* **1981**, *54*, 692. (i) Duonghong, D.; Serpone, N.; Graetzel, M. *Helv. Chim. Acta* **1984**, *67*, 1012. (j) Gulino, D. A.; Drickamer, H. G. *J. Phys. Chem.* **1984**, *88*, 1173. (k) Serpone, N.; Pelizzetti, E.; Graetzel, M. *Coord. Chem. Rev.* **1985**, *64*, 225. (l) Watanabe, T.; Fujishima, A.; Honda, K. In *Energy Resources Through Photochemistry and Catalysis*; Graetzel, M., Ed.; Academic: New York, 1983; and references cited therein. (m) Furlong, D. N.; Wells, D.; Sasse, H. F. *J. Phys. Chem.* **1986**, *90*, 1107.

(5) (a) Breddels, P. A.; Blasse, G. *Chem. Phys. Lett.* **1981**, *79*, 209. (b) Borgarello, E.; Kalyanasundaram, K.; Okuno, Y.; Graetzel, M. *Helv. Chim. Acta* **1981**, *64*, 1937. (c) Shimidzu, T.; Iyodo, T.; Koide, Y.; Kanda, N. *Nouv. J. Chim.* **1983**, *7*, 21. (d) Fendler, J. H. *J. Phys. Chem.* **1985**, *89*, 2730, and references cited therein. (e) Kamat, P. V.; Chauvet, J. P.; Fessenden, R. W. *Ibid.* **1986**, *90*, 1389.

(6) Desilvestro, J.; Graetzel, M.; Kavan, L.; Moser, J.; Augustynski, J. *J. Am. Chem. Soc.* **1985**, *107*, 2988.

effect of sensitizer loading on the observed efficiencies, and power curves for several different electron donors. Finally, we evaluate the feasibility of constructing a multipanel system from several such sensitized metal oxide panels in an array for photoinduced water splitting.

Experimental Section

Materials. Ruthenium(II) tris(2,2'-bipyridine-4,4'-dicarboxylic acid) (PF₆)₂ (**1**) was synthesized by the method of Whitten et al.⁷ A 3:1 molar ratio of 2,2'-bipyridine-4,4'-dicarboxylic acid and anhydrous ruthenium trichloride in 2-propanol was heated under reflux for 7 days under argon. Water was then added to the hot mixture and the solution was filtered. The filtrate was concentrated by rotary evaporation of the solvent. Upon addition of a saturated solution of NH₄PF₆, crystals of the ruthenium complex precipitated. The product was filtered, washed several times, dried, and purified by column chromatography.

Zinc tetrakis(4-carboxyphenyl)porphyrin (**2**) was synthesized by heating *meso*-tetra(4-carboxyphenyl)porphyrin (Strem Chemicals) in a dimethylformamide solution of Zn(OAc)₂ (Fisher) under reflux overnight. After cooling to room temperature, water was added and the mixture was acidified with concentrated HCl. The precipitate was filtered, washed several times with water, dried, and column chromatographed.

Hydroquinone (Kodak) was recrystallized twice from toluene before use. All solvents were Fisher spectral grade. Potassium iodide (Fisher) was used as received. Hydroquinonesulfonate (potassium salt; Aldrich) was washed with hot benzene and ethanol before use. Potassium ferrocyanide (MCB) was used as received. Durohydroquinone was prepared by reduction of duroquinone (Aldrich).⁸

Preparation of Porous Metal Oxide Electrodes. *A. TiO₂.* Polycrystalline TiO₂ was prepared by a method analogous to that of Koudelka et al.⁹ The surface of a titanium foil (Aesar; 0.025 mm thick, area = 56 cm²) which had been precleaned with 1:1:40 solution of HF/HNO₃/H₂O was wetted with freshly prepared 5% TiCl₄ (Fluka; >99%) in methanol. Excess solution was removed by tapping the foil. The resulting wet surface was hydrolyzed at room temperature in a chamber held at ~50% relative humidity. After ~30 min, the foil was baked in a furnace at 500 °C (open air) for 10–20 min. The wetting/baking procedure was repeated until about 10–12 layers of TiO₂ had been deposited. After a final annealing of the film at 600 °C for several hours, a white porous deposit of TiO₂ was evident on the surface of the foil. X-ray diffraction spectroscopy showed that the TiO₂ thus formed was >99% anatase. For TiO₂ electrodes to be used as panels, one side of the titanium foil was precleaned and sputtered with platinum (1000 Å) prior to TiO₂ deposition.

The surface area of TiO₂ was measured by two different methods. With a typical porous TiO₂ electrode, dye adsorption¹⁰ of methylene blue gave a roughness factor of 17, whereas nitrogen adsorption, evaluated by BET, gave a value of 305. This difference is undoubtedly caused by the larger size of methylene blue than that of nitrogen. Since the sensitizers more closely resemble the size of methylene blue, surface roughness measurements made by dye adsorption were routinely used.

The roughness factors obtained by dye adsorption varied from batch to batch for TiO₂ films. Typical surface roughness values for 10 TiO₂ layers varied from 17 to 110. A roughness factor of 2 was calculated for an aluminum-free TiO₂ single crystal by the same method.

B. SrTiO₃. Porous SrTiO₃ was deposited on a cross section of a titanium rod (Aesar; OD = 1.25 cm, 1–2 mm thick, area = 1.22 cm²) which had been polished with Buehler paper of de-

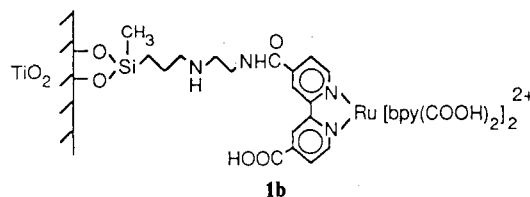
creasing coarseness (180, 240, 400, and 600 mesh, respectively) and precleaned in 1:1:50 solution of HF/HNO₃/H₂O. SrTiO₃ was prepared by a modified general method for mixed oxides.¹¹ To 100 mL of hot ethylene glycol (110 °C) was carefully added 5 mL of titanium(IV) isopropoxide (0.018 mol; Alfa; 95%), dropwise and with constant stirring. The mixture became slightly turbid after each added drop but turned clear upon stirring. The addition having been completed, 25 g of citric acid (0.12 mol) was slowly introduced into the hot mixture, producing a yellow solution. Finally 3.6 g of Sr(NO₃)₂ (0.017 mol) was carefully added to this mixture. The resulting solution was used to wet the titanium rod, which was then baked at 650 °C (open air) for 5–10 min, forming a white layer of SrTiO₃. The wetting/baking procedure was continued until about 30 layers of SrTiO₃ had been deposited. Final annealing of the film at 650 °C (open air) for 0.5 h resulted in a white ceramic film of SrTiO₃ whose formation was confirmed by X-ray diffraction. Doping of this poorly conductive SrTiO₃ in pure hydrogen at 700 °C for 2–3 h converted it to a grayish material with sufficient conductivity for use as a semiconductor electrode.

Dye Adsorption. Adsorption of **1** onto TiO₂ or SrTiO₃ was accomplished by soaking the metal oxide film in an aqueous solution of **1**, 1 × 10⁻⁴ M, at pH 3.8–4.0 for 2 h.

The resulting rusty-orange film was washed repeatedly with water. The complex appeared to adhere well to the surface even after several washings. The amount of **1** adsorbed was determined by soaking the dye-loaded electrode in a known volume of 1 M NaOH for at least 1 h, after which the UV-vis absorption spectrum of the resulting solution was obtained. The observed optical density and the extinction coefficient of **1** in 1 M NaOH ($\epsilon = 2.6 \times 10^4 \text{ M}^{-1} \text{ cm}^{-1}$ at $\lambda = 464 \text{ nm}$)¹² were used to calculate the amount of adsorbed **1**.

Adsorption of **2** was accomplished by spreading a small volume of a solution of **2** in acetone or methanol on the metal oxide surface. The solvent was then allowed to evaporate, leaving a layer of adherent porphyrin. Desorption of **2** from the surface was achieved in 1 M NaOH. From the optical density of the desorbed solution and the extinction coefficient of **2** in 1 M NaOH (ϵ 331 210, 12 233, and 9678 M⁻¹ cm⁻¹ at $\lambda = 426, 564, \text{ and } 606 \text{ nm}$, respectively)¹³ the amount of adsorbed **2** was calculated.

Covalent attachment of **1** was accomplished via a silane linking agent. Silanization of the TiO₂ surface was performed by suspending a film above a refluxing solution of dry toluene (under vacuum) containing 4-*N*-(2-aminoethyl)(3-aminopropyl)-methyltrimethoxysilane (Petrarch System, Inc.) for 2 days. Amidization of the surface-modified TiO₂ was carried out by activating **1** by treatment with 1 equiv of 1,3-diisopropyl carbodiimide (Aldrich) in dry THF under argon. The silanized TiO₂ film was allowed to soak in the resulting anhydride solution overnight. Methanol was then added to quench unreacted carbodiimide. A light rusty-orange color developed on the TiO₂ film **1b**, indicative of the presence of **1**.



Instrumentation. UV-visible spectra were obtained on a Hewlett-Packard Model 8450-Å diode array spectrophotometer.

(7) (a) Sprintschnik, G.; Sprintschnik, H. W.; Kirsch, P.; Whitten, D. J. *Am. Chem. Soc.* **1977**, *99*, 4947. (b) DeLaive, P.; Foreman, T.; Gianotti, C.; Whitten, D. *Ibid.* **1980**, *102*, 5627.

(8) Vogel, A. In *Practical Organic Chemistry*, 3rd ed.; Longman Group: London, 1974; pp 749.

(9) Koudelka, M.; Monnier, A.; Sanchez, J.; Augustynski, J. *J. Mol. Catal.* **1984**, *25*, 295.

(10) (a) Giles, C. H.; D'Silva, A. P. *Trans. Faraday Soc.* **1969**, *65*, 2516. (b) Fu, Y.; Hansen, R. S.; Bartell, F. E. *J. Phys. Chem.* **1948**, *52*, 374.

(11) Kalyanasundaram, K.; Vlachopoulos, N.; Krishnan, V.; Monnier, A.; Graetzel, M., submitted for publication.

(12) A value of $1.96 \times 10^4 \text{ M}^{-1} \text{ cm}^{-1}$ has been reported for the isopropyl ester by Duonghong, D.; Serpone, N.; Graetzel, M. *Helv. Chim. Acta* **1984**, *67*, 1012. A value of $3.76 \times 10^5 \text{ M}^{-1} \text{ cm}^{-1}$ has been reported for the Soret band at pH 6.8 by Pasternack et al. *Inorg. Chem.* **1973**, *11*, 2606; a value of $4.05 \times 10^5 \text{ M}^{-1} \text{ cm}^{-1}$ has been reported by Graetzel and co-workers.¹²

(13) (a) Kurien, K. C.; Robins, P. A. *J. Chem. Soc. B* **1970**, 855. (b) Atherton, N. M.; Cranwell, P. A.; Floyd, A. J.; Haworth, R. D. *Tetrahedron* **1967**, *23*, 1653.

TABLE I: Quantum Efficiencies for Sensitization of TiO₂ by 1 and 2

sensitizer	γ_{\max} , nm	curr ^a dens, $\mu\text{A}/\text{cm}^2$	curr ^b eff $\times 10^2 \pm 0.02$, (e out/photons in) $\times 100$	ϵ_s , ^c cm^2/mol	Γ , ^d mol/cm^2	opt ^e dens, AU	FL, ^f %	Φ
1a	460	18	0.89	$(3.2 \pm 1.7) \times 10^7$	3.0×10^{-10}	9.6×10^{-3}	2.2	41
		16	0.82		4.1×10^{-10}	1.3×10^{-2}	2.9	28
		15	0.74		4.7×10^{-10}	1.5×10^{-2}	3.4	22
1b	460	10.8	0.04	$(5.1 \pm 3.3) \times 10^8$	1.1×10^{-10}	3.5×10^{-3}	0.8	5.1
		2a	420		1.0	0.07	8.0×10^{-11}	4.1×10^{-2}
2a	420	1.7	0.11	$(5.1 \pm 3.3) \times 10^8$	1.7×10^{-10}	8.7×10^{-2}	18	9.5
		1.0	0.06		2.5×10^{-10}	1.3×10^{-1}	25	3.4
		1.1	0.07		3.0×10^{-10}	1.5×10^{-1}	29	3.6

^a Current densities were corrected for TiO₂ absorption before calculating current efficiencies at each γ_{\max} . ^b Intensities were 4.53, 5.32, and 3.45 mW/cm² at $\gamma_{\max} = 420$ and 460 nm, respectively. ^c ϵ_s = extinction coefficient of adsorbed sensitizer on TiO₂/glass in solid phase; ϵ for solution can be converted to units of cm²/mol by multiplying it by 1000 cm²/L. ^d Sensitizer. ^e OD = $\epsilon_s \Gamma$. ^f FL = fraction of light absorbed by sensitizer layer on TiO₂ film; FL = $1 - 10^{-(\text{OD})}$.

For TiO₂ electrodes, monochromatic light was supplied with an Oriel Model 7340 source equipped with a 150-W high-pressure Xe lamp, a Model 7052 photodiode detector head, and a Model 7072 detection system. Steady-state photolyses of the dye-coated TiO₂ electrodes were carried out by using a focused 1000-W high-pressure Xe lamp equipped with a water jacket, a Pyrex focusing lens, and a glass filter to exclude excitation wavelengths shorter than 420 nm. The intensity of incident light was measured with a Scientech disk calorimeter power meter (Model 36-0001) calibrated (94.3 mV/W) for full scale reading.

Metal sputtering of the titanium films was carried out with a Material Research Model 8620 sputtering system. X-ray diffraction spectra of the polycrystalline TiO₂ and SrTiO₃ films were obtained on a Philips APD 3520 X-ray diffractometer equipped with a Philips PW 1729 X-ray generator. BET surface area measurements were conducted with a Micrometrics surface analyzer instrument.

Photocurrent Measurements. Photoelectrochemical experiments were conducted in a three-compartment cell equipped with a quartz optical flat window in which the Pt flag counter electrode and SCE reference electrodes were separated from the irradiated working electrode by glass frits. All solutions were thoroughly degassed with Ar and contained 0.01 M electrolyte. Photocurrent measurements were made on a Princeton Applied Research Model 173 potentiostat/galvanostat, Model 175 programmer, and a Houston Model 2000 X-Y recorder. Action spectra for the dye-coated TiO₂ electrode (at 0.1 V vs SCE using a platinum counter electrode) were obtained by sending the output of a 150-W high-pressure Xe lamp through an Oriel 7240 grating monochromator and recording the resulting steady-state photocurrent. Intensities were measured with a vacuum photodiode radiometer or a Scientech disk calorimeter. The illuminated area of the dye-coated TiO₂ electrodes varied from 0.35 to 1.8 cm² as noted in Table I. The action spectrum for the dye-coated SrTiO₃ electrode (at 0.1 V vs SCE using a platinum counter electrode) was obtained by sending the output of a 150-W high-pressure XBO Xe arc lamp (Photon Technology International) through a Jarrel-Ash Model 82560 grating monochromator equipped with an Inco step-function Model 00141 speed-reduction motor (for continuous scanning) and by recording the resulting steady-state photocurrent on a BD90 Kipp & Zonen X-Y recorder. The illuminated area of the dye-coated SrTiO₃ electrode was 0.72 cm².

Results and Discussion

A. TiO₂. When the dye-loaded TiO₂ electrodes immersed in aqueous hydroquinone solution were irradiated with monochromatic light, a photocurrent action spectrum is produced which resembles the absorption spectral characteristics of the corresponding sensitizer (Figure 1). The observation of photocurrent at wavelengths at which bare TiO₂ is unresponsive demonstrates sensitization by 1 and 2, presumably by injecting electrons into the TiO₂ conduction band. Figure 2 illustrates the currently accepted mechanism of photosensitization of a wide-band-gap semiconductor by an adsorbed dye. Irradiation of the dye promotes the ground state (D) to its excited state (D*). If D* is sufficiently energetic (i.e., if the excited-state oxidation potential

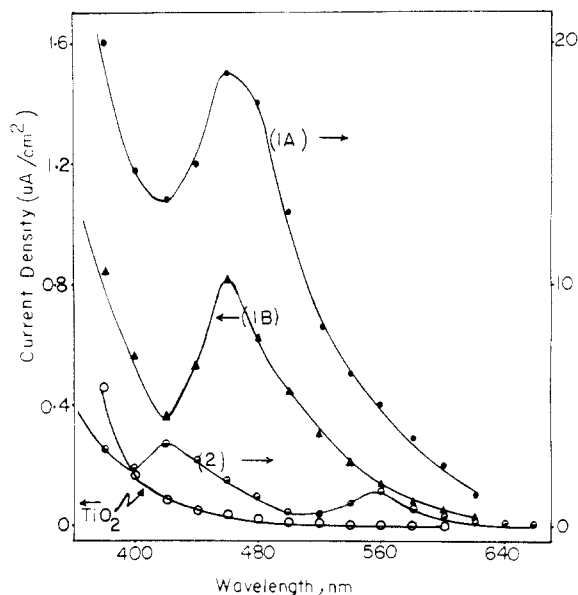
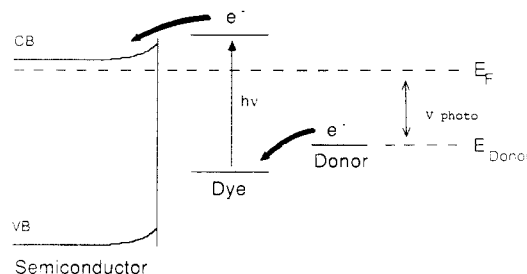


Figure 1. Photocurrent action spectra of polycrystalline anatase TiO₂ sensitized by 1 and 2. Spectrum 1A for adsorbed 1 on TiO₂ (surface loading 3.0×10^{-10} mol/cm²), spectrum 1B for chemically bonded 1 to TiO₂ (surface loading 1.1×10^{-10} mol/cm²), and spectrum 2 for adsorbed 2 on TiO₂ (surface loading 3.0×10^{-10} mol/cm²). Aqueous 10^{-3} M hydroquinone in 10^{-2} M NaCl, pH 2.6, 0.1 V (vs SCE). Illuminated areas were 0.35, 0.48, and 1.80 cm² for (1A), (1B), and (2). Light intensities were 4.53, 5.32, and 3.45 mW/cm² at $\lambda = 420, 460,$ and 560 nm, respectively.



$$V_{\text{photo}} = E_F - E_{\text{Donor}}$$

Figure 2. Dye photosensitization of a wide-band-gap n-type semiconductor.

lies at a more negative potential than the semiconductor conduction band edge), the excited dye will transfer an electron to the conduction band, producing the oxidized dye D⁺.

The requirements for efficient sensitized interfacial electron transfer are severe: (a) the rate for electron transfer from D* must be fast relative to the lifetime of excited dye; (b) no significant degradation of the excited dye or of the oxidized D⁺ may take place; and (c) a suitable donor must be present to reduce

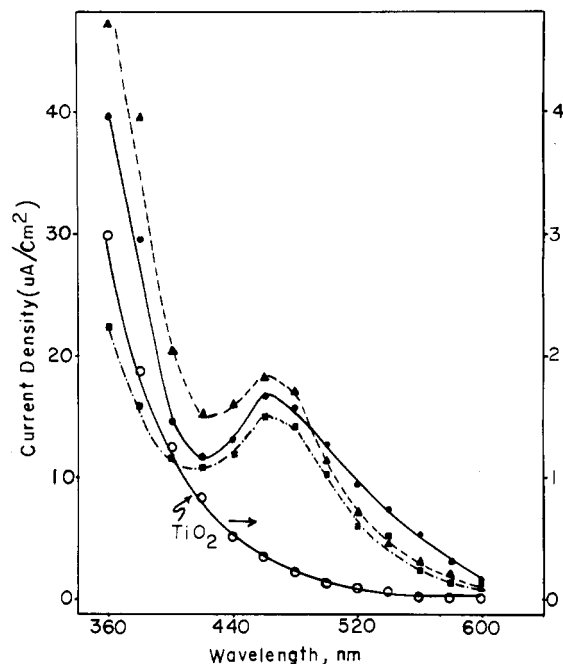


Figure 3. Photocurrent action spectra of polycrystalline anatase TiO_2 sensitized by **1** as a function of concentration of **1** on the surface. Surface loadings were 3.0×10^{-10} (\blacktriangle), 4.1×10^{-10} (\bullet), and 4.7×10^{-10} mol/cm 2 (\blacksquare). Illuminated areas were 0.35, 0.35, and 1.80 cm 2 , respectively. Other conditions were identical with those of Figure 1.

the oxidized dye back to its ground state more rapidly than D^+ is quenched by back electron transfer from the semiconductor surface states. Because dye lifetimes are short, the first condition can be met only by adsorbing or attaching the sensitizer (dye) molecule to the surface of semiconductor so that diffusion of the excited dye to the SC is unnecessary. On this modified surface, only the first adsorbed dye layer will be effective, since thicker layers form insulating barriers.¹⁴ Monolayer coverage in turn necessitates a dye with a high extinction coefficient for efficient light harvesting.

The quantum efficiency for the conversion of incident light energy to photocurrent for our dye-loaded electrodes is summarized in Table I: we find $\sim 41\%$ efficiency at $\lambda = 460$ nm for adsorbed **1** (surface loading 3.0×10^{-10} mol/cm 2) and 5.1% for covalently attached **1** (surface loading 1.10×10^{-10} mol/cm 2). A conversion efficiency of 9.5% at $\lambda = 420$ nm was observed for **2** (surface loading 1.7×10^{-10} mol/cm 2).

The values reported in Table I were obtained by measuring the observed photocurrent density (CD) induced by a light-chopped incident monochromatic source. Current efficiency (CE)¹⁶ was calculated from:

$$\text{CE} = \frac{1240(\text{CD})}{\lambda_{\text{max}} I} 100$$

in which the intensity of incident light (I) at the blazed monochromator wavelength was read from a radiometer and/or a disk calorimeter. Extinction coefficients for the adsorbed dyes ϵ_s were calculated from measured absorption of defined quantities of dye on TiO_2 -coated glass. From the ϵ_s and the loading level Γ , obtained by dye desorption and quantitation from homogeneous solution, were calculated the optical densities of the dye-loaded metal oxide surfaces. From the optical density can be calculated the fractional absorption of incident light (FL) from Beer's law:

$$\text{FL} = 1 - 10^{-(\text{OD})}$$

Finally, the quantum efficiency could be obtained as the ratio of

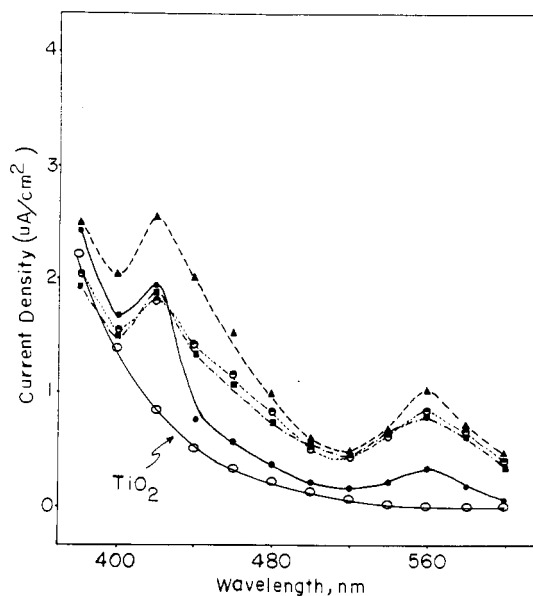


Figure 4. Photocurrent action spectra of polycrystalline anatase TiO_2 sensitized by **2**. Surface loadings of **2** were 8.0×10^{-11} (\bullet), 1.7×10^{-10} (\blacktriangle), 2.5×10^{-10} (\circ), and 3.0×10^{-10} mol/cm 2 (\blacksquare), respectively. Illuminated area was 1.80 cm 2 ; other conditions were the same as those in Figure 1.

current efficiency to fractional light absorption.

The effect of increasing dye loading on the photocurrent action spectra of **1** and **2** is shown in Figures 3 and 4. The quantum efficiency decreases as the surface coverage increases above $\sim 1 \times 10^{-10}$ mol/cm 2 (Table I summarizes results observed for coverages ranging from 3.0×10^{-10} to 4.7×10^{-10} mol/cm 2). Monolayer coverage for Degussa P25 anatase TiO_2 has been reported to be $\sim 3 \times 10^{-10}$ mol/cm 2 .^{4m} If we assume that monolayer coverage for our TiO_2 lies at approximately this value, then the observed decrease in efficiency as the surface loading exceeds monolayer coverage implies either enhanced self-quenching of excited **1** or **2** by ground-state molecules at the higher local concentration or restricted charge transfer from outer layers of dye to the electrode. When the surface coverage drops to less than a monolayer, a smaller fraction of the incident light will be absorbed, reducing incident light absorption and hence photocurrent production. The diminished efficiency of covalently attached **1** could be caused by the introduction of an insulating barrier (the silanating agent) between **1** and the TiO_2 surface.

It is reasonable to expect that optimal efficiency would be attained with highly porous metal oxide films with high surface area and surface roughness onto which monolayer coverages of dye could be adsorbed. A key difference in efficiency observed with our sensitized electrode and those recently described by Graetzel and co-workers^{15,16} thus appears to lie in the method of preparation of the metal oxide films where better light harvesting is obtained with films of high surface roughness and high fractal dimension. The higher resistance of our smoother films could also reduce observable photocurrent productions.

If the energetics for electron injection are favorable, little excited-state degradation of the dye will occur. Instead, most dye degradation occurs from D^+ , whose stability is usually assured only with rapid capture of the oxidized dye by an appropriate donor. To maximize the efficiency of reductive recovery of the oxidized dye, an optimal electron donor must be chosen. Figure 5 shows the power curves for **1a** using five donors. Values for open-circuit photovoltage (OCPV) and short-circuit photocurrent (SCPC) for each donor are reported in Table II. Tolerable fill factors were observed with each donor, but only low current efficiencies were attained. Although KI, hydroquinone, and $\text{K}_4\text{Fe}(\text{CN})_6$ give reasonable OCPV and SCPC values, both inorganic salts appear to be unattractive choices for prolonged irradiation because potassium iodide produces I_3^- which is yellow and absorbs competitively with the sensitizer in the visible and

(14) Gerischer, H. *Ber. Bunsen-Ges. Phys. Chem.* **1973**, *77*, 771.

(15) Kalyanasundaram, K.; Vlachopoulos, N.; Krishnan, V.; Monnier, A.; Graetzel, M. *J. Phys. Chem.* **1987**, *91*, 2342.

(16) Vlachopoulos, N.; Liska, P.; Augustynski, J.; Graetzel, M. *J. Am. Chem. Soc.*, in press.

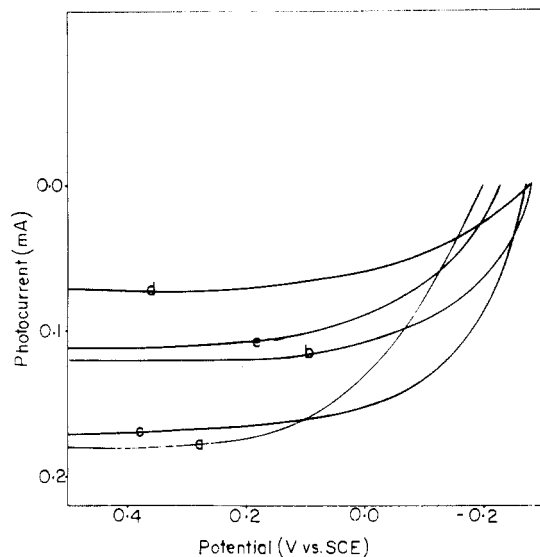


Figure 5. Power curves for sensitization of TiO_2 by adsorbed **1**. Conditions: curve a (aqueous 10^{-2} M hydroquinone), curve b (aqueous 10^{-2} M potassium iodide), curve c (aqueous 10^{-2} M potassium ferrocyanide), curve d (aqueous 10^{-2} M durohydroquinone), curve e (aqueous 10^{-2} M hydroquinonesulfonate), pH 2.6, surface loading 2.8×10^{-10} mol/cm 2 , $\lambda > 420$ nm. Incident light intensities varied from 510 to 660 mW/cm 2 .

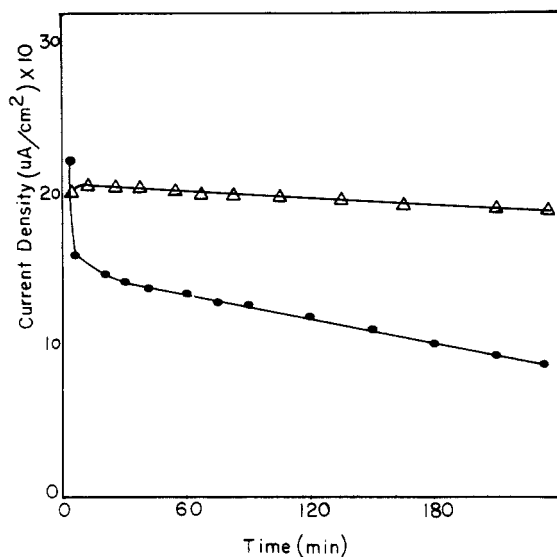


Figure 6. Dependence of photocurrent on irradiation time. Polycrystalline TiO_2 with adsorbed **1** as sensitizer, held at 0.1 V (SCE). Conditions: aqueous 10^{-2} M hydroquinone, 10^{-2} M NaCl, pH 2.6 (●), 10^{-2} M hydroquinone and 10^{-2} M NaCl in 80:20 ethanol/ H_2O (Δ), $\lambda_{\text{ex}} > 420$ nm, illuminated area was 4.9 cm 2 , and light flux was 112 mW/cm 2 .

because potassium ferrocyanide decomposes rapidly upon irradiation. Results with potassium ferrocyanide are further complicated by formation of a complex with TiO_2 .¹⁵ Thus, among the donors tested, hydroquinone in aqueous ethanol represents the best compromise electron donor for steady-state irradiation experiments.

Steady-state photocurrent was monitored as a function of irradiation time to assess the durability of **1** as a photosensitizer. Prolonged irradiation of **1** in a degassed aqueous solution containing 10^{-2} M hydroquinone and sodium chloride (electrolyte) at pH 2.6 resulted in a decrease in steady-state photocurrent (Figure 6). The initial value of the observed photocurrent could never be restored, even after a fresh solution of hydroquinone was introduced. Furthermore, after several hours of irradiation, a brownish-black film formed on the surface of **1**-loaded TiO_2 . When a similar study was carried out in a solution of hydroquinone containing 20% (by volume) ethanol, the photocurrent remained nearly constant during the entire course of irradiation (Figure 6).

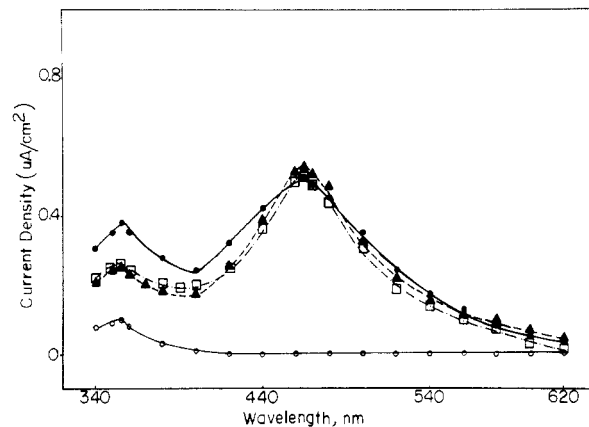


Figure 7. Photocurrent action spectra of doped SrTiO_3 sensitized by **1**. Surface loadings were 5.9×10^{-11} (▲), 1.0×10^{-10} (□), and 1.3×10^{-10} mol/cm 2 (●) and naked SrTiO_3 (○). Illuminated area was 0.72 cm 2 . Intensity at $\lambda = 465$ nm was 0.58 mW/cm 2 .

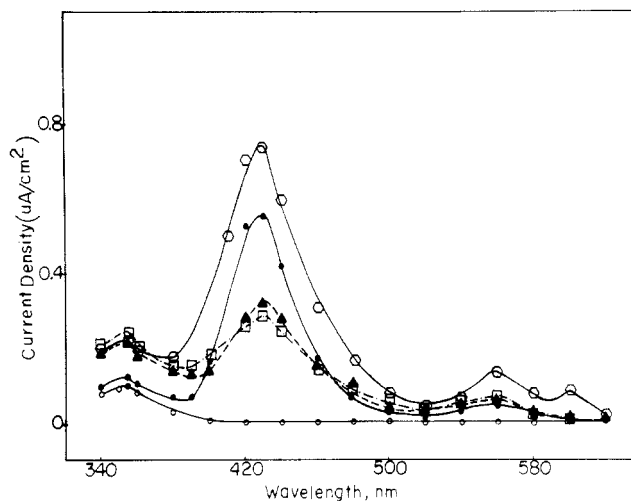


Figure 8. Photocurrent action spectra of doped SrTiO_3 sensitized by **2**. Surface loadings were 5.0×10^{-12} (□), 1.4×10^{-11} (○), 2.1×10^{-11} (●), and 2.3×10^{-11} mol/cm 2 (▲) and naked SrTiO_3 (○). Illuminated area was 0.72 cm 2 . Intensities were 0.58 and 0.44 mW/cm 2 at $\lambda = 430$ and 565 nm, respectively.

In addition, in aqueous ethanol no change in the color of the electrode was observed after a comparable irradiation time.

1,4-Benzoquinone, formed by oxidation of hydroquinone, has been reported to convert photochemically in water to 2-hydroxy-1,4-benzoquinone, which in turn polymerizes to give an insoluble brownish-black polymer which has the properties of the so-called humic acid.¹³ The decreased photocurrents observed with aqueous hydroquinone are thus consistent with the formation of a light-filtering polymer that slowly coats the electrode surface, producing a continuous drop in photocurrent. Since this polymer is soluble in ethanol,¹³ no such decrease in photocurrent would be expected in alcohol, as is observed.

B. SrTiO_3 . When SrTiO_3 monolayer-loaded with adsorbed **1** or **2** is irradiated with monochromatic light in aqueous hydroquinone solution, photocurrent action spectra parallel to the absorption spectral characteristics of the corresponding sensitizers were observed (Figures 7 and 8). Quantum efficiencies for charge injection were calculated as described earlier. Quantum efficiency on sensitized SrTiO_3 decreased as the surface coverage increased above 6×10^{-11} mol/cm 2 for **1**. With **2**, the quantum efficiency decreases as the surface coverage increases above 1×10^{-11} mol/cm 2 . (See Table III.)

Power curves (Figure 9) for undoped (curve a) and hydrogen doped (curve c) SrTiO_3 in 10^{-2} M aqueous hydroquinone (pH 2.6) were obtained. Doping improves the observed photocurrent response drastically (a factor of 30–40). However, doping also causes a larger dark current (curve b). This dark current gradually

TABLE II: Dependence of Open-Circuit Photovoltage (OCPV) and Short-Circuit Photocurrent (SCPC) on Donor's $E_{1/2}$ on Sensitized TiO_2 Electrodes^a

donor	$E_{1/2}$ vs SCE, V	electrode ^c no.	OCPV ± 0.02 , V	SCPC ± 0.5 , mA	fill factor	curr eff. ^d % $\times 10^3$
hydroquinone (HQ)	0.30	1a	0.45	0.19	0.53	8
potassium iodide (KI)	0.45		0.73	0.12	0.71	10
potassium ferrocyanide ($\text{K}_4\text{Fe}(\text{CN})_6$)	0.20		0.48	0.17	0.51	6
durohydroquinone ^b (DHQ)	0.20	1b	0.37	0.07	0.44	2
hydroquinonesulfonate (HQS)	0.09		0.33	0.11	0.40	2
HQ	0.30		0.51	0.08	0.66	4
KI	0.45	2	0.72	0.07	0.65	5
$\text{K}_4\text{Fe}(\text{CN})_6$	0.20		0.45	0.12	0.52	4
DHQ ^b	0.20		0.04	0.04	0.41	1
HQS	0.09	2	0.33	0.07	0.42	2
HQ	0.30		0.55	0.08	0.59	4
KI	0.45		0.71	0.06	0.63	4
$\text{K}_4\text{Fe}(\text{CN})_6$	0.20	2	0.47	0.07	0.30	2
DHQ	0.20		0.37	0.05	0.44	2
HQS	0.09		0.35	0.06	0.35	1

^aSolutions were 0.01 M in donor, degassed with Ar, pH 2.6, adjusted with HCl. ^b10% aqueous ethanol was used. ^c1a = 1 adsorbed on TiO_2 ; 1b = 1 covalently attached to TiO_2 ; 2 = 2 adsorbed on TiO_2 . Irradiated surface was 1.8 cm^2 ; intensity varied from 510 to 660 mW; $\lambda > 420$ nm; light source was a 1000-W high-pressure Xe lamp. ^dAll values were corrected for light absorption by solution.

TABLE III: Quantum Efficiencies for Sensitization of Doped SrTiO_3 by Adsorbed 1 and 2^a

sensitizer	γ_{max} , nm	curr dens, $\mu\text{A}/\text{cm}^2$	curr ^b eff $\times 100 \pm 0.02$, e out/photons in	ϵ_s , cm^2/mol	Γ , mol/ cm^2	opt dens, AU	FL, %	Φ
1	465	0.54	0.25	$(3.2 \pm 1.7) \times 10^7$	5.9×10^{-11}	1.9×10^{-3}	0.44	57
		0.51	0.23		1.0×10^{-10}	3.3×10^{-3}	0.76	30
		0.51	0.23		1.3×10^{-10}	4.2×10^{-3}	0.95	24
2	430	0.28	0.16	$(5.1 \pm 3.3) \times 10^8$	5.0×10^{-12}	2.6×10^{-3}	0.60	27
		0.74	0.37		1.4×10^{-11}	7.0×10^{-3}	1.6	23
		0.55	0.27		2.1×10^{-11}	1.1×10^{-2}	2.4	11
		0.69	0.34		2.3×10^{-11}	1.2×10^{-2}	2.7	13

^aCurrent densities were corrected for SrTiO_3 absorption before calculating current efficiencies at each λ_{max} . ^bIntensities were 0.58 and 0.44 mW/ cm^2 at $\lambda_{\text{max}} = 430$ and 465, respectively.

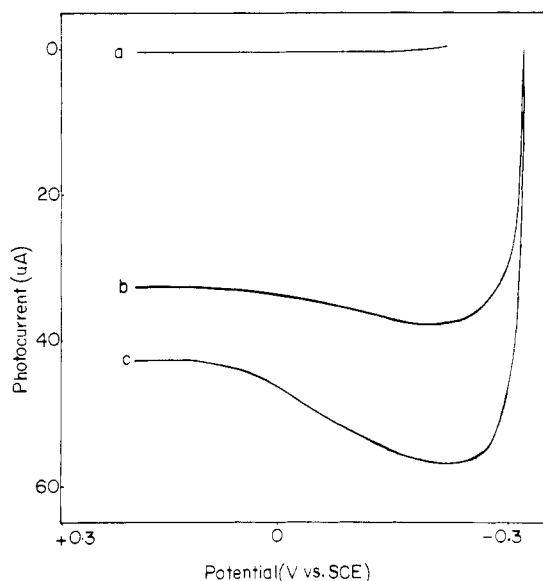


Figure 9. Power curves for (a) undoped, (b) doped in the dark, and (c) doped in the light SrTiO_3 in aqueous 10^{-2} M hydroquinone and 10^{-2} M LiClO_4 at pH 2.6. Intensity at $\lambda > 420$ nm was 490 mW/ cm^2 .

decayed toward zero with time. Since pinholes could not be detected, we speculate that the dark current may be caused by surface oxidation of highly reduced SrTiO_3 or other unknown surface-bound redox couples. The highly doped SrTiO_3 film caused direct oxidation of hydroquinone at an onset potential of about +0.3 V vs SCE. A comparison of the OCPV and SCPC values for doped SrTiO_3 (0.55 V and 0.01 mA) with those of TiO_2 (0.45 V and 0.19 mA) in hydroquinone suggest that, despite good OCPV, short-circuit photocurrent is considerably lower for SrTiO_3 , thus making it less attractive than TiO_2 as a component in a sensitized metal oxide photoelectrochemical cell.

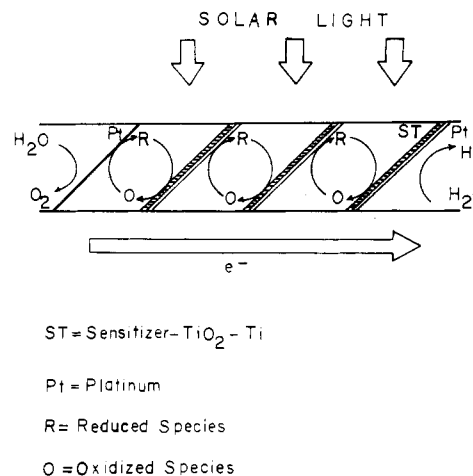


Figure 10. A multipanel water-splitting device showing three such panels arranged series.¹

TABLE IV: Observed Open-Circuit Photovoltages and Short-Circuit Photocurrents for Identically Prepared Panels (1-6) for 1a Adsorbed on TiO_2 on Plantinized Titanium^a

panel no.	int, mW	light flux, mW/ cm^2	OCPV, V	SCPC, mA	fill factor	curr eff, % $\times 10^2$
1	360	240	0.48	0.69	0.55	5.0
2	390	260	0.49	0.57	0.54	3.8
3	350	233	0.42	0.23	0.64	1.8
4	360	240	0.45	0.28	0.60	2.1
5	360	240	0.44	0.49	0.61	3.6
6	380	253	0.49	0.61	0.60	4.7

^aSolution: 0.01 M hydroquinone at pH 2.6, degassed with Ar, $\lambda > 420$ nm, light source 1000-W high-pressure Xe lamp; area of each electrode was 3.2 cm^2 but only a masked circle of 1.5 cm^2 was irradiated.

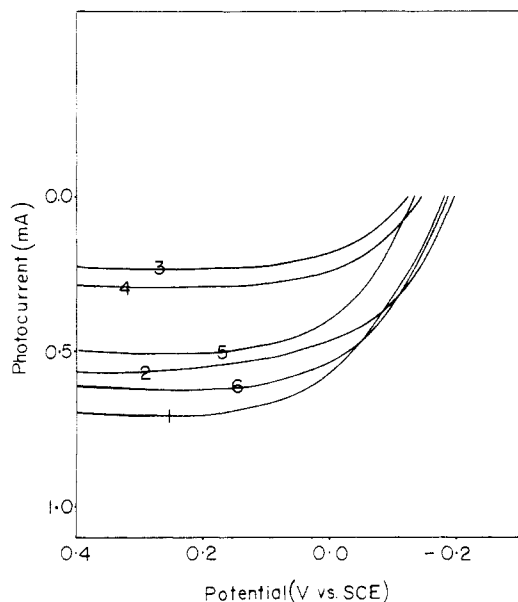


Figure 11. Power curves for **1** adsorbed on TiO_2 ; panels 1-6. Conditions: $\lambda_{\text{ex}} > 420 \text{ nm}$; illuminated area was 3.2 cm^2 ; aqueous hydroquinone (0.01 M) at $\text{pH } 2.6$.

Multipanel Devices. To evaluate the feasibility of sensitization in the construction of a multipanel water splitting device, several identical dye-loaded TiO_2 panels, backed by sputtered Pt, were employed in the previously described apparatus (Figure 10).¹ Power curves obtained for a multipanel array employing six such panels in aqueous hydroquinone solution ($\text{pH } 2.6$) are shown in Figure 11. The optimal values for OCPV and SCPC for each panel, along with the calculated fill factors and current efficiencies, appear in Table IV. These results indicate that although the observed OCPV for an individual panel is fairly good, the SCPC

is disappointingly low. Although the photovoltages were additive (when the panels were arranged in series so that enough photovoltage for water cleavage could be attained with six panels), the observed photocurrent for such an array cannot exceed that observed for the least photoconductive component, thus rendering the system impractical for construction of a visible-light-responsive water-splitting device.⁶

Summary

In summary, quantum efficiencies for the conversion of light to electrical energy have been obtained for dye-loaded TiO_2 and SrTiO_3 electrodes. For TiO_2 these values represent lower limits for quantum efficiency for sensitization (lowering of incident light intensity by a factor of 10 increased the quantum efficiency of charge injection by a factor of ~ 2). It is conceivable that the lower current efficiencies observed for our TiO_2 films are caused by reduced porosity or higher resistivity in these thick films.¹⁷ Presumably other highly absorptive dyes could also be employed, no unique advantages having been seen with **1** or **2**. Despite good OCPV values observed for both **1** and **2**, short-circuit photocurrents are too low to allow the successful sensitization of these photoelectrodes in the construction of a multipanel device that could be utilized for the photoinduced decomposition of water by visible light.

Acknowledgment. This work was supported by the Gas Research Institute. We gratefully acknowledge the gift of aluminum-free TiO_2 single crystals from Dr. A. J. Nozik (Solar Energy Research Institute, Golden, CO) and thank Professor M. Graetzel (Ecole Polytechnique, Lausanne) for helpful discussions on unpublished results and for a sample of **1**.

Registry No. **1**, 99837-92-0; **2**, 27647-84-3; DHQ, 527-18-4; HQS (potassium salt), 21799-87-1; HQ, 123-31-9; KI, 7681-11-0; TiO_2 , 13463-67-7; SrTiO_3 , 12060-59-2; $\text{K}_4\text{Fe}(\text{CN})_6$, 13943-58-3.

(17) Doping of one of our TiO_2 films in a hydrogen atmosphere at 450-500 °C improved the photocurrent by a factor of about 10.

Strong Metal-Support Interaction in $\text{Ni}/\text{Nb}_2\text{O}_5$ and Ni/TiO_2 Catalysts[†]

G. Sankar, S. Vasudevan, and C. N. R. Rao*

Solid State and Structural Chemistry Unit, Indian Institute of Science, Bangalore-560 012, India
(Received: February 18, 1987; In Final Form: September 10, 1987)

EXAFS studies of $\text{Ni}/\text{Nb}_2\text{O}_5$ and Ni/TiO_2 catalysts reduced at 773 K show evidence for the presence of a short Ni-Nb (Ti) and a long Ni...Nb (Ti) bond. The results provide evidence for considerable structural reorganization of the support in the vicinity of the Ni particles.

Introduction

Increasing interest has been evinced in the past few years in strong metal-support interaction (SMSI) catalysts,^{1,2} but the exact nature of the species responsible for their unusual catalytic activity is far from being understood. SMSI catalysts generally have oxide supports containing a reducible metal ion such as Ti^{4+} or Nb^{5+} . Several models have been proposed to explain SMSI, and these include electronic interaction between the metal particles and a suboxide formed on the support³ and alloy formation.⁴ It is well-known that extended X-ray absorption fine structure (EXAFS) can provide evidence for a metal-metal bonding in the dispersed catalysts.⁵⁻⁸ We have employed EXAFS to examine

possible evidence for SMSI in reduced $\text{Ni}/\text{Nb}_2\text{O}_5$ and Ni/TiO_2 catalysts. For this purpose, we have made use of the additive relation of the EXAFS function as well as residual spectra.^{9,10}

(1) Baker, R. T. K.; Tauster, S. J.; Dumesic, J. A., Eds. *Strong Metal-Support Interactions*; American Chemical Society: Washington, DC, 1986; ACS Symp. Ser. No. 298.

(2) Imelik, B.; Naccache, C.; Coudutier, G.; Praliaud, H.; Meriquedeau, P.; Gallazot, P.; Martin, G. A.; Verdine, J. C., Eds. *Metal Support and Metal-Additive Effects in Catalysis*; Elsevier: New York, 1982.

(3) Tauster, S. J.; Fung, S. C. *J. Am. Chem. Soc.* **1978**, *100*, 415.

(4) Horsley, J. A. *J. Am. Chem. Soc.* **1979**, *101*, 2870.

(5) Tzou, M. S.; Teo, B. K.; Sachtler, W. M. H. *Langmuir* **1986**, *2*, 773.

(6) Beard, B. C.; Ross, P. N. *J. Phys. Chem.* **1986**, *90*, 6811.

(7) Sakellison, S.; McMillan, M.; Haller, G. L. *J. Phys. Chem.* **1986**, *90*, 1733.

(8) Koningsberger, D. C.; Martens, J. H. A.; Prins, R.; Short, D. R.; Sayers, D. E. *J. Phys. Chem.* **1986**, *90*, 3048.

[†]Contribution No. 423 from the Solid State and Structural Chemistry Unit.

* To whom all correspondence should be addressed.